

Hybrid Mutation Particle Swarm Optimisation Method for Available Transfer Capability Enhancement

H. Farahmand¹, M. Rashidinejad², A.A. Gharaveisi², A. Mousavi³, M.R. Irving³, and G.A. Taylor³

¹ SINTEF Energy Research, Trondheim, Norway (Hossein.Farahmand@sintef.no)

²Shahid Bahonar University of Kerman, Kerman, IRAN

³Brunel Institute of Power Systems (BIPS), Electronic and Computer Engineering, School of Engineering and Design, Brunel University, UK

ABSTRACT:

A Hybrid Mutation Particle Swarm Optimisation (HMPSO) technique for improved estimation of Available Transfer Capacity (ATC) as a decision criterion is proposed in this paper. First, this is achieved by comparing a typical application of the Particle Swarm Optimisation (PSO) technique with conventional Genetic Algorithm (GA) methods. Next, a multi-objective optimisation problem concerning optimal installation and capacity allocation of Flexible AC Transmission Systems (FACTS) devices is presented and demonstrated.

Modern heuristic techniques such as PSO have been demonstrated to be suitable approaches in solving non-linear power system problems. The outcome of this research further demonstrates that with better utilisation of FACTS devices, it is possible to improve transmission capabilities.

The motivation of this research is a direct consequence of the deregulation of electricity industries and power markets worldwide. The current deregulated environment provides transmission systems operators (TSO) with more options when procuring transmission services.

The effectiveness of the proposed algorithm is demonstrated across a range of case studies, and the results are validated through analyses conducted on IEEE 30-bus and 57-bus test systems.

1 INTRODUCTION

The liberalisation of electricity markets has created the need for researchers and practitioners to put forward better power systems optimisation techniques [1]. The open access to transmission networks enables international involvement in the global electrical power supply markets. The market forces and resultant squeeze on profit margins demand better utilisation of the existing transmission facilities [2,3]. Improvements to Available Transfer Capability (ATC) in power transmission systems are constrained by relatively low voltages and heavily loaded circuits and buses. FACTS devices offer a versatile alternative to conventional reinforcement methods through increased flexibility, lower cost and reduced environmental impacts. They provide new control facilities, both in steady state power flow control and dynamic stability control. Static VAR Compensator (SVC) and Thyristor Controlled Series

Compensator (TCSC) are the popular FACTS devices for effective parallel and series compensation in order to enhance ATC.

The capacity of transmission equipment can be improved without resorting to costly installation of new transmission networks. This can be achieved by prudent deployment of FACTS devices in the transmission system [4, 35]. The deployment of series and parallel reactive compensators would improve ATC. Typically an optimisation method determines the capacity and the location of these compensators [5, 36]. The multi objective optimisation problem that deals with deployment of FACTS devices in a network is able to handle conflicting objectives at different power system operation modes. The objectives in this paper include ATC enhancement, voltage profile improvement and active power losses reduction. Moreover, the objectives are constrained by power flow limits, network reliability and system security [3,6].

Particle Swarm Optimisation (PSO) [7, 37] is applied in this paper to solve the problem of installation and capacity allocation of FACTS devices in the power transmission network. Over the last decade, PSO algorithms have been successfully deployed in power system optimisations studies [8-12, 38]. One of the advantages of PSO is the capability of particles to share information among each other. For example, during a search process the particles can benefit from the discoveries and previous experiences of all other particles with solution information in the system, which in turn leads to higher overall solution speed. However, due to the multimodality of the objective function, the former advantage could seriously harm the search for a global optimal solution. The multi objective function may also degrade the diversity criteria of the algorithm, and reduce the global searching capability of the PSO algorithm [13].

In order to overcome this weakness and improve the overall solution process, a novel Hybrid Mutation PSO (HMPSO) method consisting of a standard PSO method and a new mutation operator is proposed in this paper. The proposed hybrid method combines fuzzy logic and the Analytical Hierarchy Process (AHP) to model the qualification of each problem objective [28], and prioritise of the objectives. The fitness evaluation applies the velocity of each particle to the global optimum point. A mutation operator that initiates artificial diversification in the particle population is embedded in the PSO to prevent premature convergence to a local optimum.

In the following section, the definition of the problem and the resultant mathematical formulation is discussed. In section 3, an introduction to PSO and the novel HMPSO method is given. In section 4, the model is validated across a range of case studies followed by analysis of results. Section 5, outlines the concluding remarks.

2 PROBLEM DEFINITION AND MATHEMATICAL MODELLING

This research focuses on a multi-objective optimisation problem. The problem is formulated in order to find the best location and capacity of FACTS devices. The objective function includes the enhancement of Available Transfer Capability (ATC), the maintenance of the voltage profile and minimisation of active power losses.

2.1 PROBLEM DEFINITION AND MODELLING

The most important goal is to enhance ATC with respect to the economical constraints

of a typical interconnected network. In order to achieve this goal, a formal definition of ATC as well as its role in power system operation and control is presented in the first step.

2.1.1 Available Transfer Capability

According to the North American Electric Reliability Council (NERC), ATC is the difference between Total Transfer Capability (TTC) and the summation of the Existing Transmission Commitment (ETC), the Transmission Reliability Margin (TRM) and the Capacity Benefit Margin (CBM) [15]:

$$ATC = TTC - (ETC + TRM + CBM) \quad (1)$$

The TTC is the largest transfer increase between the selected source and sink with no violation of any security constraints or contingency [14].

In order to calculate the TTC, the thermal and voltage limits are also considered. The three most practical and popular methods for calculating TTC are:

- i. Repeated Power Flow (RPF) method [15].
- ii. Continuation Power Flow (CPF) method [16].
- iii. Security Constrained Optimal Power Flow (SCOPF) method [17].

The method adopted in this research to calculate TTC is based on a simple implementation of the RPF method, which is a suitable method for large-scale power systems in comparison with the other methods [4]. The RPF method needs to trace PV curve up to the nearest distance to the 'nose' point (at the nose point the RPF method will diverge). This offers the possibility of considering voltage stability in TTC calculation. In accordance with the RPF method, the system load and power generation will be increased by a specified rate. The power increase continues until at least one of the system constraints related to TTC are violated. Variations in the real power generation and demand of each bus are shown in Equations (2) and (3).

$$P_{Gi} = P_{Gi}^{\circ} (1 + \lambda k_{Gi}) \quad (2)$$

$$P_{Di} = P_{Di}^{\circ} (1 + \lambda k_{Di}) \quad (3)$$

Where:

- P_{Gi} : increased real power generation at bus i
- P_{Gi}° : original real power generation at bus i
- P_{Di} : increased real load demand at bus i.
- P_{Di}° : original real load demand at bus i.
- λ : scalar parameter.
- k_{Gi} : constant rate of changes in generation as λ varies.
- k_{Di} : constant rate of changes in load as λ varies.

The reactive power demand (Q_D) is also increased in accordance to fix the power factor for all loads.

Therefore, TTC can then be calculated using the Equation (4). The equation shows the maximum loadability of an electric power system before reaching the voltage collapse point along with the maximum exchange flows on interfaces, which have not violated the capacity limitation. Thereby, voltage limits and thermal limits are considered in TTC calculation. The TTC calculation is based on static consideration and does not account for the dynamic stability limitations.

$$TTC = \min \left[\left(\sum_{i \in k} P_{Di}(\lambda_{\max}) - \sum_{i \in k} P_{Di}^o \right), \sum_{ij \in \text{Tie Lines}} P_{Maxij} \right] \quad (4)$$

Where, $\sum_{i \in k} P_{Di}(\lambda_{\max})$ is the sum of the load in sink area at $\lambda = \lambda_{\max}$, $\sum_{i \in k} P_{Di}^o$ is the sum of the load in sink area when $\lambda = 0$, and $\sum_{ij \in \text{Tie Lines}} P_{Maxij}$ is the sum of tie-lines capacity between the send and the sink area.

The existing committed transmission (ETC) is calculated using the power flow calculation. The transmission reliability margin (TRM) is treated as a constant percentage (i.e. 10%) of the TTC. The capacity benefit margin (CBM) can be based on the market value between energy contractors. For the sake of simplicity, CBM is assumed to be zero. Based on the above assumptions, ATC can be estimated by the Equation (5).

$$ATC = TTC - ETC - TRM = (1 - k)TTC - ETC \quad (5)$$

Where, k is a predefined percentage of the calculated TTC. Voltage profile and active power losses are calculated using the power flow solution.

2.1.2 Static VAR Compensator (SVC) Model

In the steady state case, an SVC can be modelled as a reactive power injection/absorption illustrated in Equation (6) [18]:

$$Q_{SVC} = V_t(V_t - V_{ref})X_{SL} \quad (6)$$

Where: X_{SL} is the voltage control, V_t is the terminal voltage and V_{ref} is the reference voltage. Equation (7) can be used as the alternative representation of Equation (6):

$$Q_{SVC} = B_{SVC} \times V_{ref}^2 \quad (7)$$

Here the value of B_{SVC} varies between the minimum and the maximum capacitive and inductive susceptance. This range is more than the desired reactive power that can be maintained.

2.1.3 Thyristor Controlled Series Compensator (TCSC) Model

Transmission lines are generally modelled using the classical π model with lumped parameters. The series compensator TCSC is a static capacitor or reactor with an impedance of jX_c as shown in Figure 1.

Figure 1- Equivalent Circuit of Line with TCSC

The difference between the line susceptance before and after the inclusion of a TCSC can be expressed as Equation (8)[19].

$$\Delta y_{ij} = y'_{ij} - y_{ij} = (g_{ij} + jb_{ij})' - (g_{ij} + jb_{ij}) \quad (8)$$

Where:

$$g_{ij} = \frac{r_{ij}}{2} \frac{r_{ij}}{r_{ij} + x_{ij}} \quad \text{and} \quad b_{ij} = -\frac{x_{ij}}{2} \frac{x_{ij}}{r_{ij} + x_{ij}}$$

$$g'_{ij} = \frac{r_{ij}}{2} \frac{r_{ij}}{r_{ij} + (x_{ij} + x_c)} \quad \text{and} \quad b'_{ij} = -\frac{x_{ij} + x_c}{2} \frac{x_{ij} + x_c}{r_{ij} + (x_{ij} + x_c)}$$

By deployment of a TCSC between Bus i and Bus j in a power system, the admittance matrix Y_{bus} can be modified as follows:

$$Y'_{bus} = Y_{bus} + \begin{bmatrix} 0 & 0 & 0 & \dots & 0 & 0 & 0 \\ 0 & \Delta y_{ij} & 0 & \dots & 0 & -\Delta y_{ij} & 0 \\ 0 & 0 & 0 & \dots & 0 & 0 & 0 \\ \dots & \dots & \dots & \dots & \dots & \dots & \dots \\ 0 & 0 & 0 & \dots & 0 & 0 & 0 \\ 0 & -\Delta y_{ij} & 0 & \dots & 0 & \Delta y_{ij} & 0 \\ 0 & 0 & 0 & \dots & 0 & 0 & 0 \end{bmatrix} \quad (9)$$

2.2 THE MATHEMATICAL FORMULATION

Two control variables in this problem are the location and the level of compensation for SVC and TCSC. These variables are applied to the objective function and constraints as they are simultaneously deployed in the power flow equations. The SVC and the TCSC are deployed as series and parallel FACTS devices. The objective functions and constraints can be formulated as follows:

$$\begin{aligned}
& \text{Optim} \{ O_{\text{ATC}}, O_{\text{Voltage}}, O_{\text{Loss}} \} \\
& \left. \begin{aligned}
& P_{Gi} - P_{Di} - \sum_{j=1}^N |V_i| |V_j| (G_{ij\text{-FACTS}} \cos \delta_{ij} + B_{ij\text{-FACTS}} \sin \delta_{ij}) = 0 \quad i = 1, \dots, N \\
& Q_{Gi} - Q_{Di} - \sum_{j=1}^N |V_i| |V_j| (G_{ij\text{-FACTS}} \sin \delta_{ij} - B_{ij\text{-FACTS}} \cos \delta_{ij}) = 0 \quad i = 1, \dots, N \\
& |V_i|_{\min} \leq |V_i| \leq |V_i|_{\max} \quad i = 1, \dots, N \\
& S_{ij} \leq S_{ij}^{\max} \quad i, j = 1, \dots, N \\
& P_{G_{\min}} \leq P_{Gi} \leq P_{G_{\max}} \quad i = 1, \dots, N_G \\
& Q_{G_{\min}} \leq Q_{Gi} \leq Q_{G_{\max}} \quad i = 1, \dots, N_G \\
& Q_{\min}^{\text{SVC}} \leq Q^{\text{SVC}} \leq Q_{\max}^{\text{SVC}} \\
& X_{\min}^{\text{TCSC}} \leq X^{\text{TCSC}} \leq X_{\max}^{\text{TCSC}}
\end{aligned} \right\} \quad (10)
\end{aligned}$$

Where:

- O_{ATC} : ATC value
- O_{voltage} : voltage profile
- O_{Loss} : active power losses
- P_{Gi} : real power generation at bus i
- Q_{Gi} : reactive power generation at bus i
- P_D : real power demand
- Q_{Di} : reactive power demand at bus i .
- N : number of buses in the system.
- $|V_i|$ and $|V_j|$: voltage magnitudes at bus i, j .
- $G_{ij\text{-FACTS}}$ and $B_{ij\text{-FACTS}}$: real and the imaginary parts of the ij^{th} element of Y_{bus} admittance matrix including FACTS devices
- S_{ij} : actual power flow in line ij
- $S_{ij \max}$: thermal limit of line ij
- N_G : number of generators
- $P_{G_{\max}}, P_{G_{\min}}$: the maximum and the minimum real power generation at bus i .
- $Q_{G_{\max}}, Q_{G_{\min}}$: the maximum and the minimum reactive power generation at bus i .
- Q_{svc} : SVC capacity (MVar). (The capacity of SVC is kept between Q_{\min}^{SVC} and Q_{\max}^{SVC} , where it is assumed that $Q_{\min}^{\text{SVC}} = -200$ MVar and $Q_{\max}^{\text{SVC}} = 500$ MVar)
- X^{TCSC} : reactance of TCSC (TCSC is modelled as a capacitor with minimum compensation X_{\min}^{TCSC} , which is supposed to be zero and maximum compensation X_{\max}^{TCSC} , which is limited up to 60% of line reactance where TCSC will be located)

3 PARTICLE SWARM OPTIMISATION

Heuristic methods in general are suitable for solving combinatorial multi-object optimisation problems. These methods are called “*intelligent*” since the move from one

solution to another is achieved using logical reasoning. Heuristic algorithms search for a solution within a subspace of the search region in a relatively fast computational time. However, the most important advantage of heuristic methods lies in the fact that they are not limited by restrictive assumptions in their search space. Furthermore, it is important to note that in spite of their ability to offer good results, they do not guarantee a global optimum solution. The heuristic methods for solving combinatorial multi-object optimisation problems such as Tabu Search (TS), Simulated Annealing (SA), Genetic Algorithms (GA) and Particle Swarm Optimisation (PSO) each have their advantages and disadvantages [20-22].

In this paper, the PSO method has been chosen due to its specific applicability to the described optimisation problem [7]. Similar to GA, PSO is a population-based optimisation technique. The system to be studied is initialised with a population of random solutions and the search for the optimal solution is conducted by continuously evolving generations of solutions. However, unlike GA, PSO has no evolution operators such as crossover and mutation. The potential solutions in the PSO method are called particles. The particles fly over the problem space by following current near optimum particles. Similar to GA, PSO is initialised within a population of random solutions and it seems to be superior to GA based on computational speed and less complexity in assigning system variables. The method retains information or details of good solutions provided by all particles [23]. PSO provides an environment of constructive cooperation between particles to share information. The successful application of PSO to the minimisation function [24] and feed forward neural network design [25], have demonstrated its potential in problem solving.

The individual solutions fly through the search space with adjustable velocity. The velocity can be dynamically adjusted based on the flying experience of the particle and that of its companions. At every step of the search process for the optimal solution, each particle maintains the information about its position with respect to the best solution or fitness that it has achieved so far. This value is called *pbest*. The other variable that is traced by the particle swarm optimiser is the global best value, *gbest*. The velocity of each particle toward its *pbest* and *gbest* locations is adjusted at every step of the optimisation process. The acceleration values towards *pbest* and *gbest* are generated randomly.

For nonlinear optimisation, this technique involves simulating social behaviour among particles that fly through a multidimensional search space, where each particle represents a single intersection of all search dimensions. Particles would evaluate their positions or fitness levels with respect to the objective function at each iteration. In addition, particles in local neighbourhoods share memories of their "best" positions, and then use those memories to adjust their own velocities for subsequent positions.

In the PSO algorithm the i^{th} particle X_i is defined as a potential solution in D -dimensional space, where $X_i = (x_{i_1}, x_{i_2}, \dots, x_{i_D})$. Each particle also maintains a memory of its previous best position $P_i = (p_{i_1}, p_{i_2}, \dots, p_{i_D})$ and velocity $V_i = (v_{i_1}, v_{i_2}, \dots, v_{i_D})$ along each dimension. Following each iteration, the particle vector $P = [P_1, P_2, \dots, P_n]$ is adjusted with regard to the best fitness in the local neighbourhood. This adjustment will

be implement using the “*gbest*” and the “*pbest*” factors leading to the best fitness for the population. Velocity adjustment along each dimension is described by Equation (11), where a new position for the particle can be determined [23]:

$$v_i = w \cdot v_{i-1} + c_1 \times \text{rand}(0,1) \times (x_{i_{gbest}} - x_i) + c_2 \times \text{Rand}(0,1) \times (x_{i_{pbest}} - x_i) \quad (11)$$

$$x_{i+1} = x_i + v_i$$

Where:

w is the inertia weight factor.

c_1, c_2 are the acceleration constants, $\text{rand}(0,1)$ and $\text{Rand}(0,1)$ are random numbers.

$x_{i_{gbest}}$ is the best particle among all particles in the population and $x_{i_{pbest}}$ is the best historical position for particle x_i . The constants c_1 and c_2 represent the weighting of the stochastic acceleration terms that pull each particle x_i towards $x_{i_{gbest}}$ and $x_{i_{pbest}}$ positions.

According to existing literature c_1 and c_2 are often set to be 2.05 [33-34]. In order to reduce the number of iterations required to reach the optimal solution, a suitable selection of inertia weight (w) is introduced to provide a balance between global and local explorations. The inertia weight normally decreases linearly from 0.9 to 0.4 during the optimisation process. The inertia weight can be set according to the Equation (12) [23].

$$w = w_{\max} - \frac{w_{\max} - w_{\min}}{\text{iter}_{\max}} \times \text{iter} \quad (12)$$

Where iter_{\max} is the maximum number of iterations (generations), and iter is the current number of iterations. In this study, the population size is considered 200 and $\text{iter}_{\max} = 50$.

3.1 MUTATION PARTICLE SWARM OPTIMISATION (MPSO)

One of the weaknesses of the PSO method is stagnation. Stagnation here refers to premature convergence of solutions. In a stagnated state the velocity of particles reach almost zero and the particles become tightly clustered around a point called the local optimum. The resulting tight cluster of solutions prevents the system from generating any new solutions. However, the resultant local optimum or first global best contains all the members of the swarm. By introducing a mutation to an individual member in the swarm a new global best can be achieved. This mechanism provides a means of escaping local optima and accelerating the search for the best global solution.

In this paper an arithmetic mutation operator has been deployed. This dynamic technique of non-uniform mutation has been successfully implemented in a number of other studies [22].

For a given particle P , if part P_k is selected for mutation then with equal probability either of the following can be selected:

$$\begin{cases} O_k = P_k - r(a_k + P_k)\left(1 - \frac{iter}{iter_{max}}\right)^c \\ O_k = P_k + r(b_k - P_k)\left(1 - \frac{iter}{iter_{max}}\right)^c \end{cases} \quad (13)$$

Where:

O_k is the result obtained from applying the mutation operator on the part P_k of the selected particle P , a_k and b_k are the lower and the upper band of P_k , r is a random number between (0,1) with a uniform distribution. $iter_{max}$ is the maximum number of iterations, and $iter$ is the current number of iterations. c is the parameter determining the degree of non-uniformity. In this paper the value of c is assumed to be 3. Note that this mutation is dynamic. This means that as the number of generation increases then the non-uniformity of this operator decreases. Non-uniformity of mutation is related to the amount of $\left(1 - \frac{t}{T}\right)^c$ that means by increasing 'this value trends to decrease.

Eventually when t is equal to T , this amount is zero so that O_K will be equal to P_K .

3.2 FITNESS FUNCTION

The proposed fitness function considers three objectives: (1) Improving voltage profile, (2) enhancing ATC value and (3) minimising active power losses. A hybrid technique of fuzzy logic [27] and Analytical Hierarchy Process (AHP) is used to determine the fitness value.

The Fuzzy membership functions and values adopted in this paper are described in the following equation based on the minimisation case:

$$\mu_{f_i}(\bar{X}) = \begin{cases} 1 & \text{if } f_i(\bar{X}) < f_i^{\min} \\ h_i(f_i(\bar{X})) & \text{if } f_i^{\min} \leq f_i(\bar{X}) \leq f_i^{\max} \\ 0 & \text{if } f_i(\bar{X}) > f_i^{\max} \end{cases} \quad (14)$$

Where $h_i(f_i(\bar{X}))$ in Equation (14) is a strictly linear or nonlinear monotonically decreasing function. The proposed fitness function is a weighted combination of the three objectives and can be represented as follows:

$$\text{Fitness} = \alpha_1\mu_1 + \alpha_2\mu_2 + \alpha_3\mu_3 \quad (15)$$

Where α_i is considered to be the weight of each objective and AHP is adopted here to ensure that the weighting criterion is consistent with the degree of importance of the objectives. The associated pair-wise comparison matrix can be defined as follows [28]:

$$P = [p_{ij}] = \begin{bmatrix} \frac{w_1}{w_j} \\ \frac{w_2}{w_j} \\ \vdots \\ \frac{w_k}{w_j} \\ \vdots \\ \frac{w_N}{w_j} \end{bmatrix} = \begin{bmatrix} \frac{w_1}{w_1} & \frac{w_1}{w_2} & \dots & \frac{w_1}{w_k} & \dots & \frac{w_1}{w_N} \\ \frac{w_2}{w_1} & \frac{w_2}{w_2} & \dots & \frac{w_2}{w_k} & \dots & \frac{w_2}{w_N} \\ \frac{w_1}{w_1} & \frac{w_2}{w_2} & \dots & \frac{w_k}{w_k} & \dots & \frac{w_N}{w_N} \\ \vdots & \vdots & \vdots & \vdots & \vdots & \vdots \\ \frac{w_k}{w_1} & \frac{w_k}{w_2} & \dots & \frac{w_k}{w_k} & \dots & \frac{w_k}{w_N} \\ \frac{w_1}{w_1} & \frac{w_2}{w_2} & \dots & \frac{w_k}{w_k} & \dots & \frac{w_N}{w_N} \\ \vdots & \vdots & \vdots & \vdots & \vdots & \vdots \\ \frac{w_N}{w_1} & \frac{w_N}{w_2} & \dots & \frac{w_N}{w_k} & \dots & \frac{w_N}{w_N} \\ \frac{w_1}{w_1} & \frac{w_2}{w_2} & \dots & \frac{w_k}{w_k} & \dots & \frac{w_N}{w_N} \end{bmatrix} \quad (16)$$

The weighting vector is $W = [w_1 \ w_2 \ \dots \ w_N]^T$ and the P matrix is multiplied by the vector W.

$$PW = \begin{bmatrix} \frac{w_i}{w_j} \\ \frac{w_j}{w_j} \end{bmatrix} [w_i] = \begin{bmatrix} \sum_{i=1}^N w_i \end{bmatrix} = N[w_i] \quad (17)$$

$$\therefore PW = NW \quad \& \quad (P - NI) = 0 \quad (18)$$

If all elements of P are consistent, the eigenvalues of P are equal to zero except for a nonzero eigenvalue (λ_{\max}), which is equal to the number of objectives (N). The weights can be derived by normalising the eigenvector with respect to the largest eigenvalue [28]. In the case where objectives have unequal importance, it should be ensured that alternative solutions with greater importance are more likely to have higher impact in fitness value [29]. To reflect this impact, w_i can be considered as the corresponding exponents of fuzzy membership values. With respect to the conditions set, the proposed multi-objective fitness function can be represented as [30]:

$$\text{Fitness} = \mu_{O_1}^{w_1}(x) + \mu_{O_2}^{w_2}(x) + \dots + \mu_{O_N}^{w_N}(x) \quad (19)$$

Where,

μ_{O_i} is the fuzzy membership of i^{th} objective participant in the goal function and w_j is the weight of j^{th} objective.

3.3 HYBRID MUTATION PARTICLE SWARM OPTIMISATION (HMPSO)

The solution algorithm consists of two main steps. The first step is to calculate the fitness value through a hybrid technique. The second step is to implement the PSO algorithm with mutations. This methodology can be described as a Hybrid Mutation Particle Swarm Optimisation (HMPSO) algorithm. Figure 2 shows the flow chart of the proposed HMPSO methodology.

Figure 2- HMPSO Flow Diagram

4 CASE STUDY AND ANALYSIS OF RESULTS

In this section, studies were performed on IEEE 30-bus and 57-bus test systems in order to compare the proposed HMPSO method with the established GA and standard PSO techniques. The GA techniques discussed here include; the Binary GA (BGA), Real GA (RGA) [23] and Hybrid RGA (HRGA) [4, 30]. One SVC and a TCSC are used as the FACTS devices in order to test the proposed HMPSO algorithm. The methodology is developed using the MatPower Package [31].

4.1 IEEE 30-BUS TEST SYSTEM

This system consists of 6 generators and 20 loads. The base values are assumed to be 100 MVA and 132 kV. The detailed electrical data can be found in reference [32]. To address the first objective of ATC enhancement the system is divided into areas 1 and 2. Table 1 contains the relevant data for areas 1 and 2. There is no generating power available in area 2 (i.e. the deficit area), therefore, some transmission from area 1 (surplus area) should be committed in order to compensate for the deficit area. This approach would ensure the enhancement of ATC with respect to the future growth in load. Secondly, some part of the deficit area is radially connected to the system which may compromise system security.

Table 1-IEEE 30-Bus Areas Characteristics

In order to obtain the fitness values of control variables (i.e. *particle's position* in the wording of the PSO), the ATC value from area 1 to area 2 needs to be calculated, where $ATC = 0.9 TTC - ETC$ (*Base case value*). TRM is considered to be 10% of the TTC. A predefined transfer limit condition is established at which point the transfer has been increased to such a value that there is a binding security limit. In this case, the voltage collapse at bus 26 shows a security limit binding condition. Any further power transfer in the specified direction would cause the violation of the binding limit and would compromise system security. The P-V curve in figure 3(a) illustrates the condition. The collapse occurs at bus 26 when the voltage magnitude is 0.562 pu and total active load of supposed test case is 362.5 MW.

Figure 3- P-V Curve and Voltage Profile with no FACTS Devices for Bus 26

Therefore, the resulting value of ATC in area 1 to area 2 is 89.164 MW. The details of ATC calculation has been described in [4]. The voltage profile without the minimisation of active transmission losses and with no FACTS device is equal to 17.7 MW as described in figure 3(b).

The qualitative nature of the decision criteria combines well with the fuzzy logic approach adopted here. Figure 4 shows the typical membership functions for voltage profile, desired ATC and transmission power loss. The ideal per-unit value for bus voltage lies between 0.95 and 1.1 p.u, although in this case study the values between 0.8 and 0.95 are also acceptable. This assumption is completely dependent on the operational standards of system and the values can be determined using operational expertise.

Figure 4: Fuzzy membership functions for: (a) Bus Voltages, (b) desired ATC

and (c) Transmission Power Loss

The system operator selects the desired value for ATC between the two areas. The value of ATC is assumed to be at most 120 MW, which is the total capacity of tie-lines between the areas, and at least 89.164 MW, which is equal to the exiting committed transmission. The active losses membership function shown in figure 4(c) determines the degree of satisfaction that is required to achieve this objective. This diagram also is determined using operational expertise and can be varied from case to case.

In order to determine the fitness for each particle with respect to the importance of each objective and associated constraint, the fitness value for PSO is calculated by applying a fuzzy AHP method. Within the fuzzy AHP method the level of importance of each object can be defined as:

ATC is more important than voltage profile and much more important than transmission loss. Moreover, the voltage profile would be more important than the transmission loss. Thus the weight relationship would be $W = [0.9281 \ 0.3288 \ 0.1747]^T$. This outcome can be substituted in Equation (19) resulting as Equation (20).

$$Fitness = \{ \mu_1^{0.9281}(x) + \mu_2^{0.3288}(x) + \mu_3^{0.1747}(x) \} \quad (20)$$

Based on the calculated fitness value, the next optimal position can be obtained using the HMPSO formulation. This process continues until the results converge and the terminating condition is satisfied based on a certain number of iteration (e.g. 50 iterations).

4.1.1 Comparison of GA and PSO results

Comparison of results from applying the GA and PSO algorithms to the IEEE 30-bus test case are presented in Table 2. These methods are BGA, RGA and HRGA for GA and ordinary PSO, Mutation PSO (MPSO) and HMPSO for PSO.

Table 2- Results for Different Type of GA and PSO

The observations show that by adopting the BGA, RGA, PSO and MPSO algorithms, despite obtaining substantial improvements in ATC the active power losses increase.

The HMPSO optimisation technique has its own limitations. These limitations stem from the nature of hybrid techniques, therefore, special attention needs to be paid to the properties of the fuzzy membership functions and the pair-wise comparison techniques deployed for the ATC problem.

Figure 5- Variation of the Best Fitness Value for GA, RGA and HRGA with Respect to Generation

However, Figure 5 provides evidence that using HRGA leads to better overall performance when compared to the GA method.

Figure 6- Variation of *g*best Value for PSO, MPSO and HMPSO with Respect to Generations

The graph presented in Figure 6 shows that HMPSO method provides better solutions when compared with PSO and MPSO. As illustrated in Figure 7 the *g*best value has the same role as the fitness value in GA. Furthermore, the HMPSO method has resulted in a better solution when compared with HRGA.

Figure 7- Comparison between HRGA & HMPSO

Based on the above results the HMPSO method is selected for the optimisation process.

Figure 8- Resultant Voltage Profile using GA, RGA, HRGA, PSO, MPSO, and HMPSO Methods

Comparing the voltage profile with respect to the six mentioned methods it becomes evident that deployment of HMPSO method yields better results. The contrast is more noticeable in buses 12 to 20 and 27 to 30 where the base case has the weakest voltage.

4.2 IEEE 57-BUS TEST SYSTEM

This system has 57 buses, 80 branches, 7 generators, 42 loads and total demand of 1250.8 MW. The base system values are assumed to be 100 MVA and 132 KV. The electrical data for this system can be found in [32]. The system is divided into areas 1 and 2 as described in Table 3.

Table 3-IEEE 57-Bus Areas Characteristics

The ATC value between areas 1 and 2 is equal to 309.4 MW. The voltage collapse occurs at bus 31 which is the binding security limit. Additionally, the voltage magnitude would be 0.42 p.u. and the total active load is 1317.1MW as shown in Figure 9.

Figure 9- P-V Curves for Bus 31

Two SVC and a TCSC are used as FACTS devices for the test. The best location for the first SVC is at bus 38 where the optimum capacity is 179.254 MVar. The second SVC is located at bus 29 where the capacity is 41.45 MVar. The best location of TCSC is line 9-12 where the level of compensation is equal to 60% of the expected line reactance. Hence the line reactance including TCSC decreases from 0.295 p.u. to 0.118 p.u. The voltage profile comparison is illustrated in Figure 10 showing significant improvement at buses 14 to 49 especially for bus 31 where voltage collapse occurs in accordance to load increasment.

Figure 10- IEEE 57-Bus Voltage Profile Pre and Post Deployment of FACTS Devices

The ATC has increased by 37.4% from 309.4 MW to 425.2 MW. Also the transmission active power loss reaches 32.78 MW as opposed to 47.27MW, which represents a loss reduction of 30.6%. The search process guarantees good convergence and the variation of “*gbest*” values versus number of generations required using the HMPSO algorithm is shown in Figure 11. It also shows that the proposed search process ensures fast and effective convergence.

Figure 11- Variations of *gbest* Value against the Number of RGA Generations

The results of the test show that voltage collapse violates the TTC constraints while the deployment of FACTS devices increases the voltage security margins. Table 4 shows the power flow in each line between areas 1 and 2 prior to voltage collapse. The results also clearly indicate that the capability of the system to maintain transmission power has improved.

Table 4-Power Flow of Each Tie-line Before Voltage Collapse

The PV curves for the weakest Bus-31 pre and post deployment of FACTS devices are shown in Figure 12. By utilising FACTS devices the system security margin is enhanced to the extent that the distance to nose point where the voltage collapse occurs is pro-longed. By increasing the voltage security margin, the TTC value and the ATC would eventually be enhanced.

Figure 12- PV Curves for Base Case and After Using FACTS Devices

5 CONCLUSION

The results of a research project to determine the best location for FACTS devices with respect to the optimum amount of compensation levels have been presented in this paper. This was achieved by utilising the AHP and Fuzzy sets in combination with PSO algorithms. The proposed methodology was implemented using repeated power flow procedures with respect to line thermal and voltage stability limits. Alternative GA and PSO techniques were implemented to compare the performance of each technique. The results proved the novel HMPSO method proposed in this paper to be the most promising. The results also indicate that ATC could be significantly enhanced through prudent usage of FACTS devices. IEEE 30-bus and 57-bus systems were deployed as the test cases.

The decision making optimisation method proposed in this paper will help transmission systems operators to make better decisions in their procurement of services in electric power markets. An additional advantage would be savings in the development of new lines and networks leading to a reduced impact on the environment.

REFERENCES

1. Song, Y. H. and Wang, X.: 'Operation of Restructured Power Systems', 'Operation of Market-Oriented Power System', (Springer Verlag, 2003, 1st edn, ch1,) pp 1-2.
2. Shahidehpour, M., and Alomoush, M.: 'Decision Making in a Deregulated Power Environment Based on Fuzzy Sets', 'AI Applications to Power Systems', (Kluwer Publishers, 1999).
3. Shirmohammadi, D., Wollenberg, B., Vojdani, A., Sandrin, P., Pereira, M., Rahimi, F., Schneider, T., and Scott, B.: 'Transmission Dispatch and Congestion Management in the Emerging Energy Market Structures', IEEE Trans. on Power Systems, November 1998, 13,(4), pp. 1466-1474.
4. Rashidinejad, M., Farahmand, H., Fotuhi-Firuzabad, M., and Gharaveisi, A. A.: 'A Hybrid Technique for ATC Enhancement Using TCSC', Journal of Electric Power Systems Research, January 2008, 78, (1), pp. 11-20.
5. Farahmand, H., Rashidinejad, M., Gharaveisi, A. A.: 'A Combinatorial Approach of Real GA & Fuzzy to ATC Enhancement', Turkish journal of electrical engineering & computer sciences, 2007, 1, (4), pp. 77-88.
6. Karami, A., Rashidinejad, M., Gharaveisi, A.A., and Farahmand, H.: 'Voltage Security Enhancement by Optimal FACTS Location via RGA', Proc. Technical and Physical Problems in Power Engineering, TPE-2006, Gazi University, Ankara, Turkey, May 2006, pp. 29-31,.
7. Kennedy, J. and Eberhart, R.: 'Particle Swarm optimisation' in Proc. IEEE Int. Conference on Neural Networks, 4, 27 Nov-1 Dec. 1995, pp. 1941-1948.
8. Yoshida, H., Kawata, K., Fukuyama, Y., and Nakanishi, Y.: 'A Particle Swarm Optimisation for Reactive Power and Voltage Control Considering Voltage Stability' in Proc. Int. Conference in Intelligent System Application to Power Systems, Rio de Janeiro, Brazil, 1999, pp. 117-121.
9. Fourie, P. C. and Groenword, A.: 'The Particle Swarm Optimisation Algorithm in Size and Shape Optimisation', Struct. Multidisc. Optim., 2002, Vol. 23, pp. 259-267.
10. Cockshott, A. R. and Hartman, A.: 'Improving fermentation medium for Echinocandin B production part II: Particle swarm optimisation', Process Biochem., 2001, 36, pp. 661-669.
11. Ciuprina, G., Ioan, D., and Munteanu, I.: 'Use of intelligent-particle swarm optimisation in electromagnetics' IEEE Trans. Magnetics, Mar. 2002, 38, (2, Part 1), pp. 1037-1040.
12. Sriyanyong, P.: 'Particle Swarm Optimisation with Applications in Power System Generation', PhD Thesis, Brunel Institute of Power Systems, School of Engineering and Design, Brunel University, UK, 2007.
13. Ho, S. L., Yang, S., Ni, G., Lo, E.W. C., and Wong, H. C.: 'A Particle Swarm Optimisation-Based Method for Multiobjective Design Optimisations', IEEE Trans. Magnetics, May 2005, 41, (5), pp. 1756-1759.
14. North American Electric Reliability Council (NERC), 'Available Transfer Capability Definition and Determination' (Report June 1996).
15. Ejebe, G. C., Tong, J., and Waight, J. G.: 'Available Transfer Capability Calculations', IEEE Trans. On Power Systems, Nov. 1998, 13, (No.4), pp. 1512-1527.
16. Chiang, H., Fluek, A. J., Shah, K. S., and Balu N.: 'CPFLOW : A Practical Tools

- for Tracing Power System Steady-State Stationary Behavior Due To Load and Generation Variation', IEEE Trans. on Power systems, May 1995, 10, (2). pp. 623-634.
17. Gisin, B. S., Obessis, M. V., and Mitsche, J. V.: 'Practical methods for transfer limit analysis in the power industry deregulated environment' in Proc. 21st IEEE Int. Conference in Power Industry Comput. Applicat., 1999, PICA 99, pp. 261–266.
 18. Ou, Y. and Singh C.: 'Improvement Of Total Transfer Capability Using TCSC and SVC', IEEE Power Engineering Society Summer Meeting, 15-19 July 2001, 2, pp. 944 - 948.
 19. Feng W. and Shrestha, G. B.: 'Allocation of TCSC Devices to Optimize Total Transmission Capacity in a Competitive Power Market', IEEE Power Engineering Society Winter Meeting, 28 Jan.-1 Feb. 2001, (2), pp. 587 – 593.
 20. Glover, F.: 'Tabu Search' University of Colorado, Boulder, (CAAI Report 88-3, 1988).
 21. Kirkpatrick, S., Gellat, C. D., and Vecchi, M. P.: 'Optimisation by Simulated Annealing' Science, 1983, 220, pp. 671–680.
 22. Goldberg, D. E.: 'Genetic Algorithms in Search Optimisation and Machine Learning' (Kluwer Academic Publishers, Boston, MA, 1989).
 23. Shi, Y., Eberhart, R. C.: 'A Modified Particle Swarm Optimiser' Proceedings of the 1998. Congress on Evolutionary Computation, Piscataway, 4-9 May 1998, pp.69 - 73.
 24. Shi, Y. and Eberhart, R. C.: 'Empirical Study of Particle Swarm Optimisation', Proceedings of the 1999. Congress on Evolutionary Computation, CEC 99, Piscataway, 6-9 July 1999, pp. 1945-1950.
 25. Clerc, M. and Kennedy, J.: 'The particle swarm—Explosion, stability, and convergence in a multidimensional complex space', IEEE Trans. Evol. Comput., Feb. 2002, 6, (1), pp. 58–73.
 26. Zhang, C., Shao, H., and Li, Y.: 'Particle swarm optimisation for evolving artificial network', in Proc. IEEE Int. Conf. Syst., Man, Cyber., 2000, 4, pp. 2487–2490.
 27. Wang, L.: 'Linguistic Variables and Fuzzy IF-Then Rules', 'A Course in Fuzzy Systems and Control', (Prentice Hall, 1997, Chapter 5), pp.59-72.
 28. Satty T. L.: 'A Scaling Method for Method for Priorities in Hierarchical Structure', Journal of Math Psychology, 1977, 15, pp. 234-281.
 29. Zhu, J. Z., Irving M. R.: 'Combined active and reactive dispatch with multiple objectives using an analytic hierarchical process', IEE Proc.-Gener. Transm. Distrib, July 1996, 143, (4), pp.344 – 352.
 30. Farahmand H., Rashidinejad M. and Gharevaishi, A.A.: 'An Application of Hybrid Heuristic Approach for ATC Enhancement', IEEE Large Engineering systems Conference on Power Engineering, Halifax, Canada, July 2006, pp. 125-130.
 31. Zimmermann, R.D., Gan, D.: 'MatPower: A MATLAB Power System Simulation Package, Version 3.0b3', PSERC, September 2004.
 32. IEEE 30-Node & 57-Node System, Power systems test case archive. University of Washington. [Online]. Available: <http://www.ee.washington.edu/research/pstca/> accessed 2006.
 33. Ben Ali M. Y., 'Primary Title: Psychological model of particle swarm optimization based multiple emotions', Applied Intelligence, Mar. 2011, 36, (3), pp. 649–663.
 34. Ren, B. and W. Zhong, 'Multi objective optimization using chaos based PSO', Inform. Technol. J., 2011, 10, (10), pp.1908-1916.

35. E.S. Ali, S.M. Abd-Elazim, Coordinated design of PSSs and TCSC via bacterial swarm optimization algorithm in a multimachine power system, *International Journal of Electrical Power & Energy Systems*, 36, (1), March 2012, pp. 84-92
36. M.A. Khaburi, M.R. Haghifam, 'A probabilistic modeling based approach for Total Transfer Capability enhancement using FACTS devices', *International Journal of Electrical Power & Energy Systems*, 32, (1), January 2010, pp. 12-16.
37. E. Nasr Azadani, S.H. Hosseinian, B. Moradzadeh, 'Generation and reserve dispatch in a competitive market using constrained particle swarm optimization', *International Journal of Electrical Power & Energy Systems*, 32, (1), January 2010, pp. 79-86.
38. L.D. Arya, L.S. Titare, D.P. Kothari, 'Improved particle swarm optimization applied to reactive power reserve maximization', *International Journal of Electrical Power & Energy Systems*, 32, (5), June 2010, pp. 368-374.

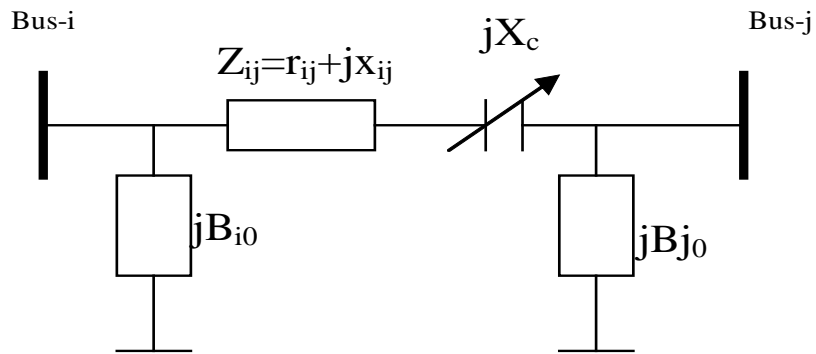


Figure 2- Equivalent Circuit of Line with TCSC

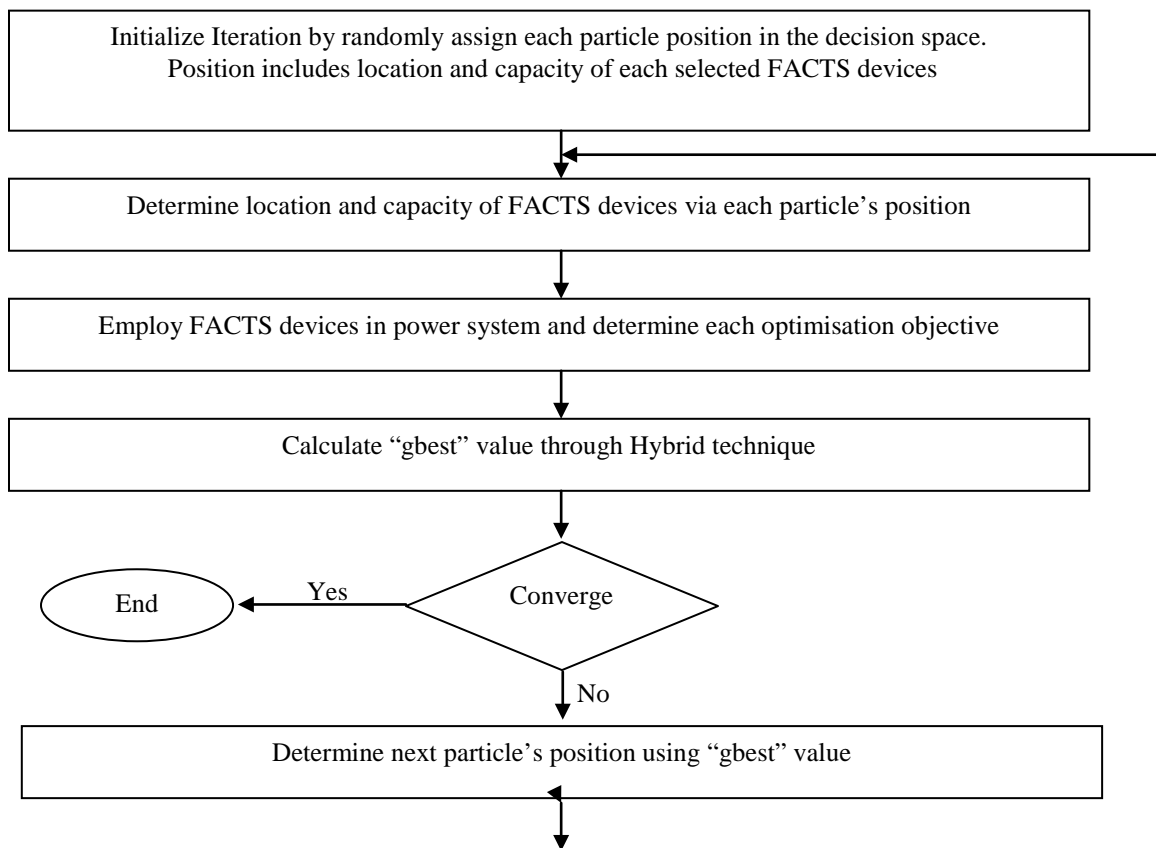
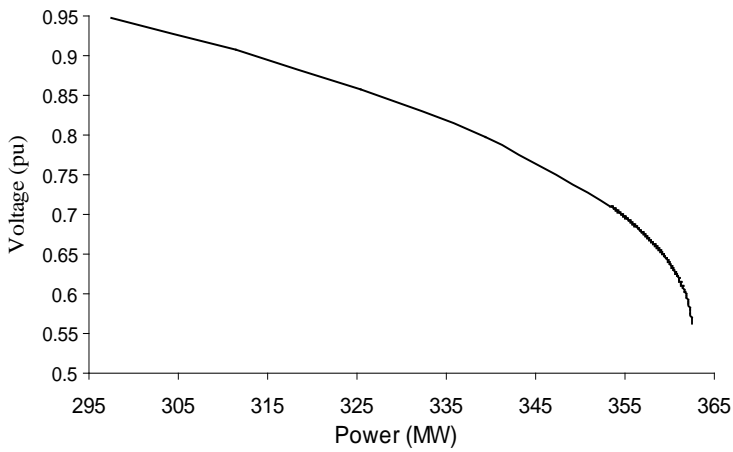
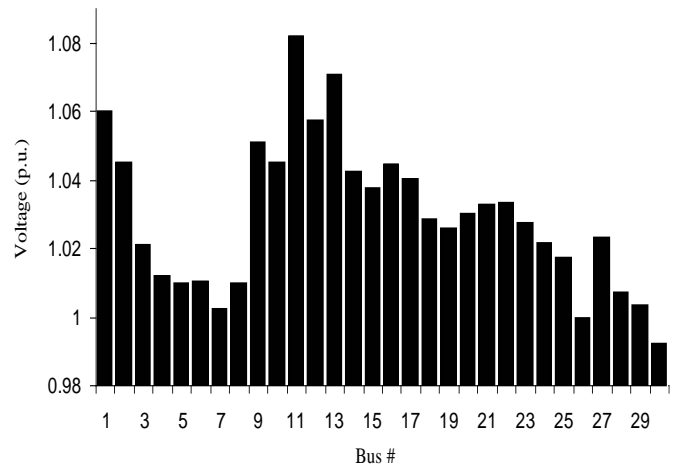


Figure 2- HMPSO Flow Diagram

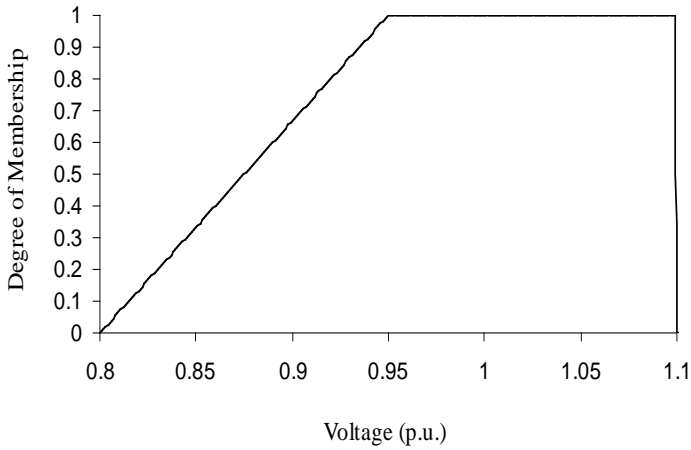


(a)

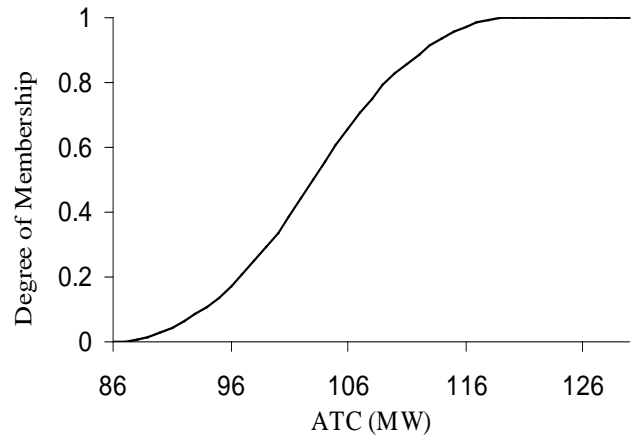


(b)

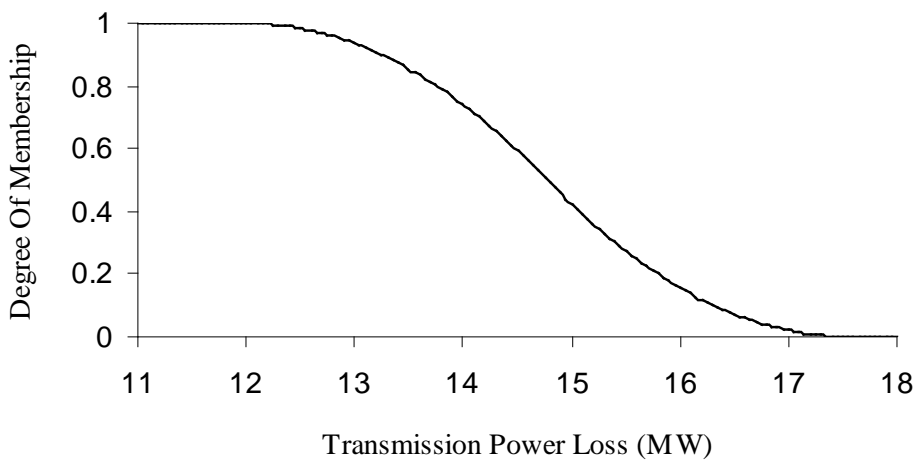
Figure 3- P-V Curve and Voltage Profile with no FACTS Devices for Bus 26



(a)



(b)



(c)

Figure 4: Fuzzy membership functions for: (a) Bus Voltages, (b) desired ATC and (c) Transmission Power Loss

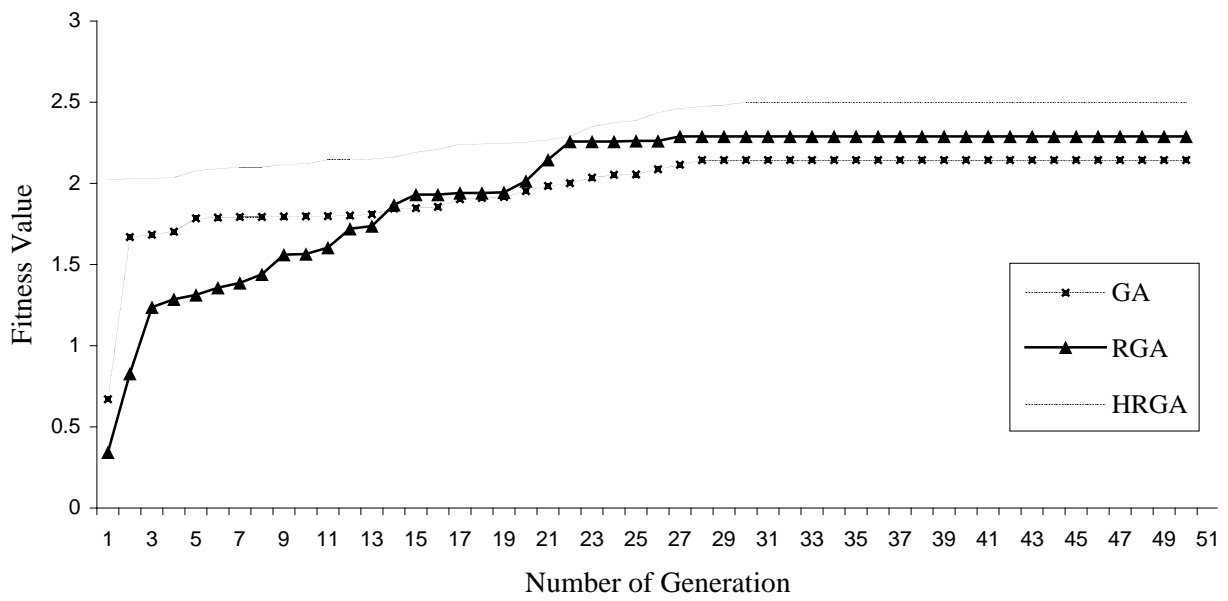


Figure 5- Variation of the Best Fitness Value for GA, RGA and HRGA with Respect to Generation

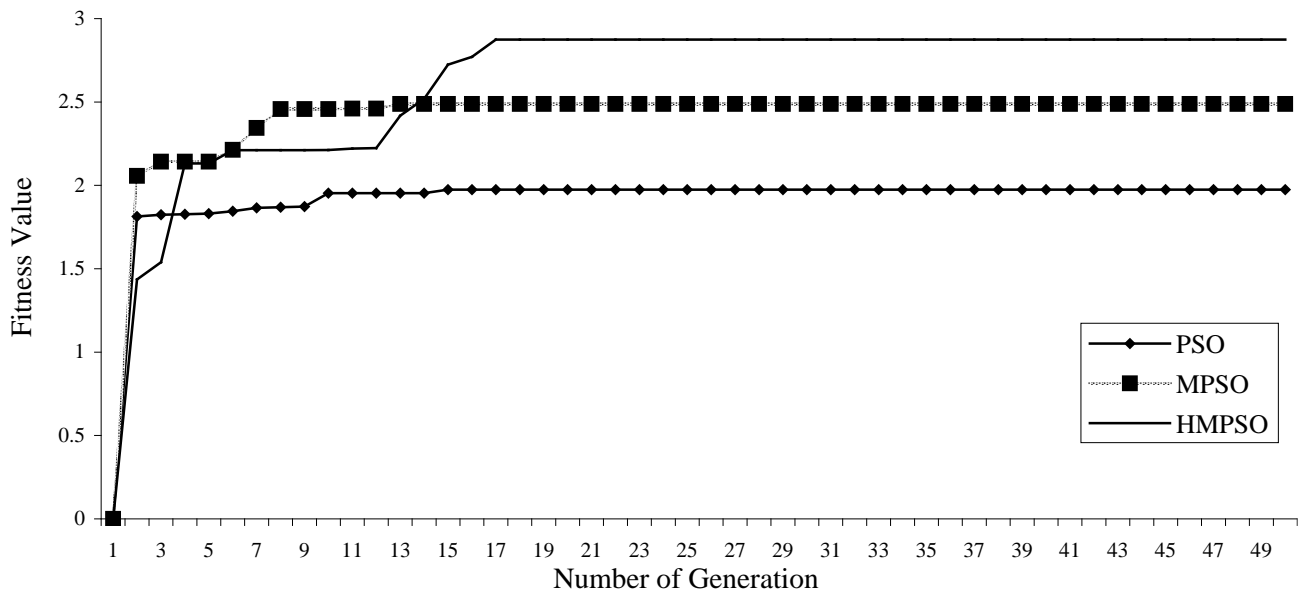


Figure 6- Variation of *gbest* Value for PSO, MPSO and HMPSO with Respect to Generations

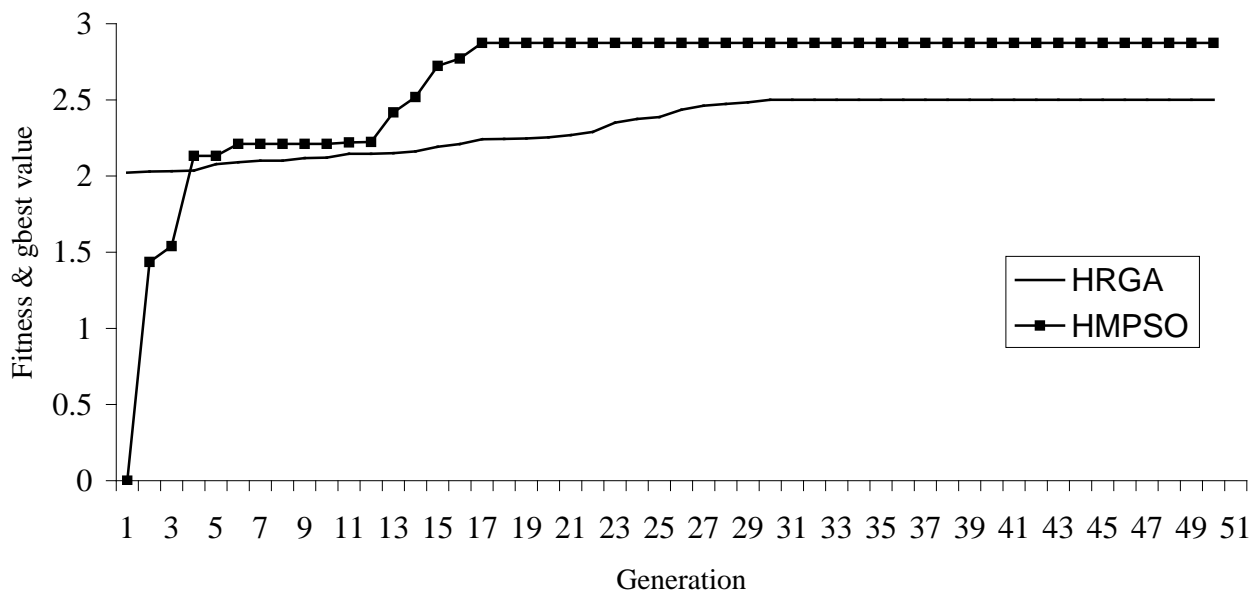


Figure 7- Comparison between HRGA & HMPSO

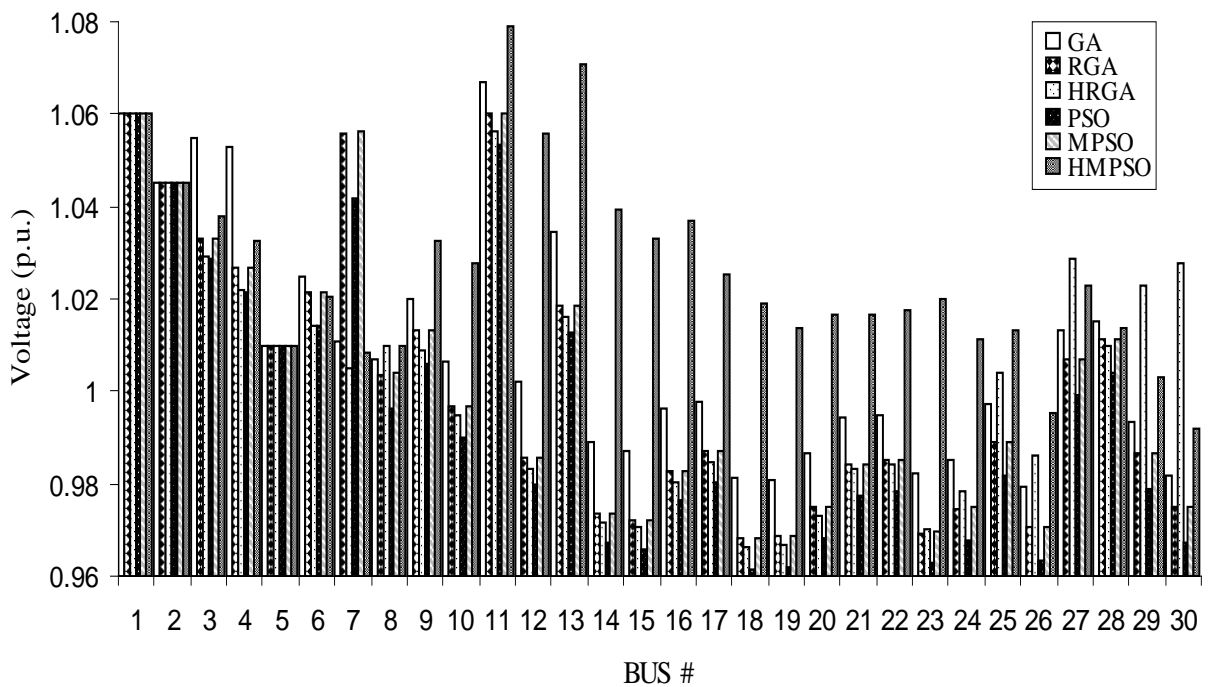


Figure 8- Resultant Voltage Profile using GA, RGA, HRGA, PSO, MPSO, and HMPSO Methods

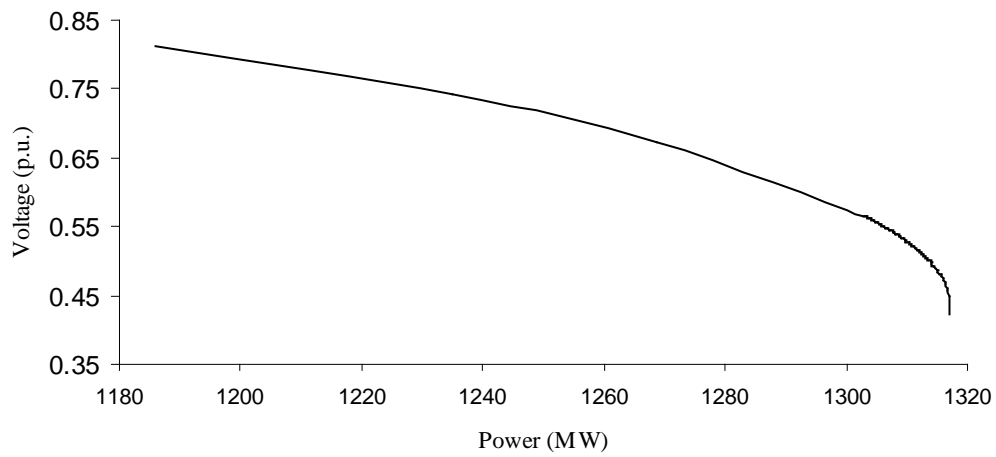


Figure 9- P-V Curves for Bus 31

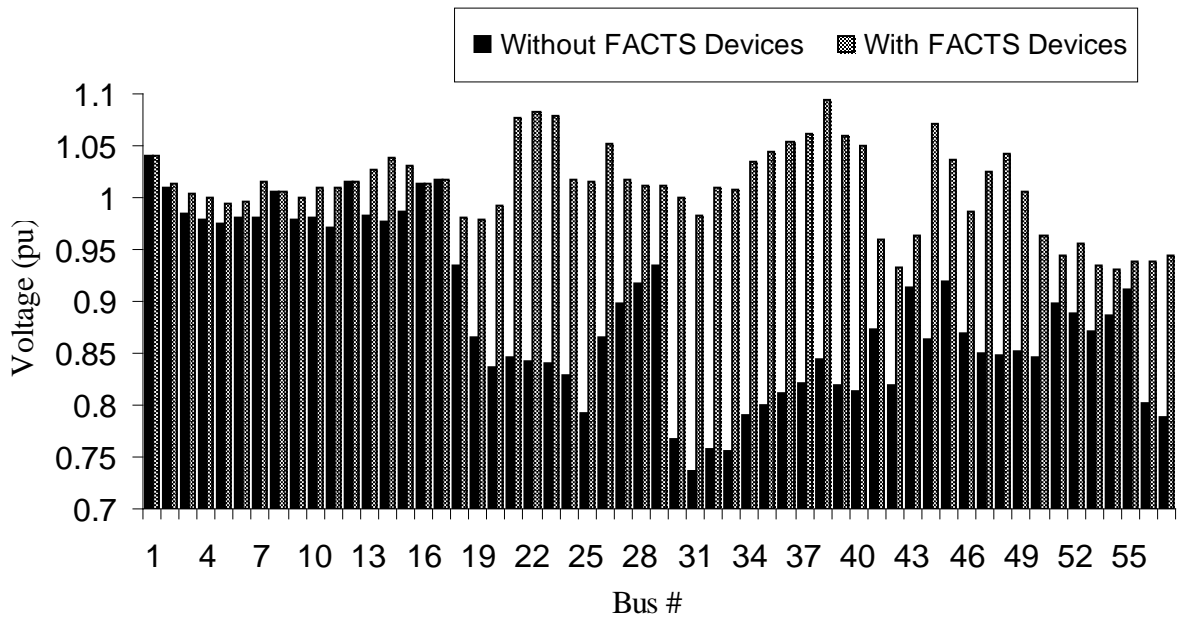


Figure 10- Comparing the Voltage Profile Before and After Employment of FACTS Devices

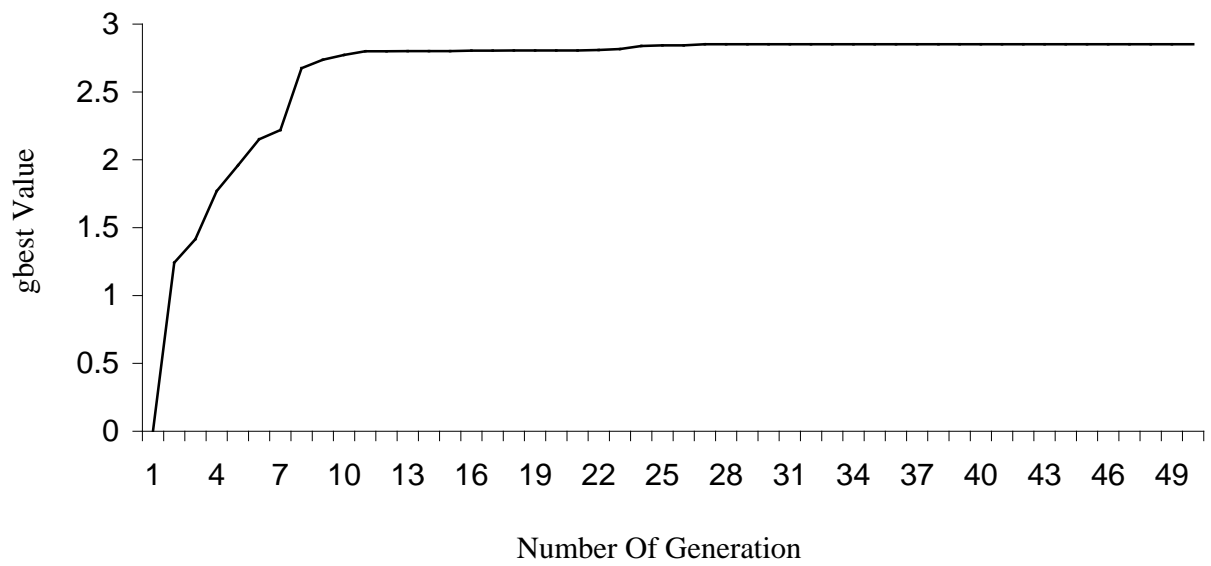


Figure 11- Variations of *gbest* Value against the Number of RGA Generations

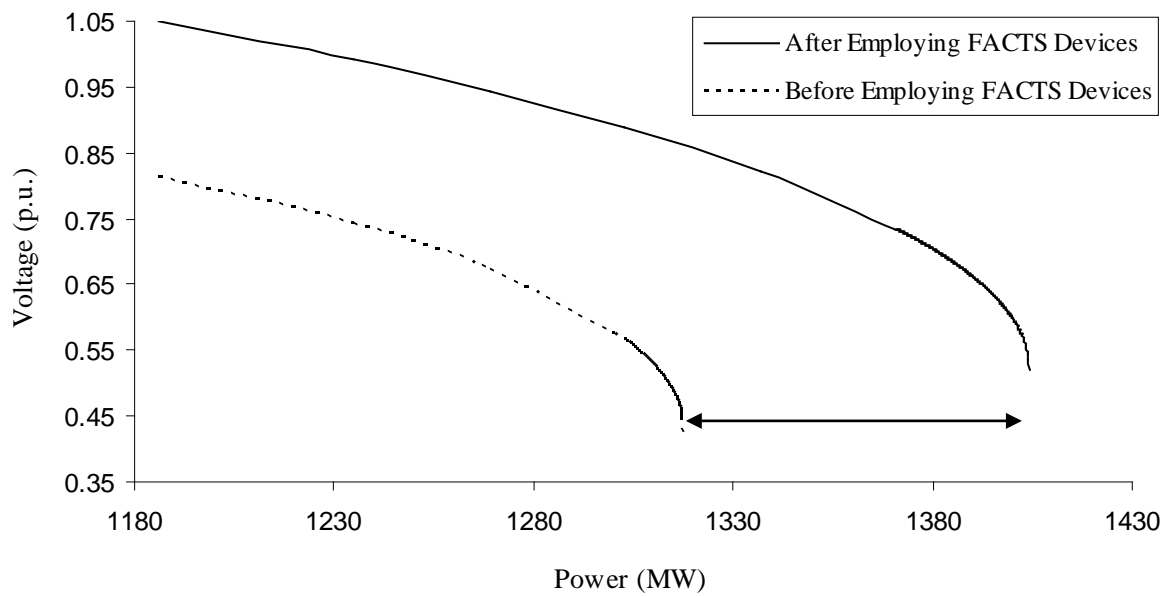


Figure 12- PV Curves for Base Case and After Using FACTS Devices

Table 5-IEEE 30-Bus Areas Characteristics

Area	Bus numbers	Generation (MW)	Load (MW)
1	1,2,3,4,5,6,7,8,9,11,12,13	301.65	189.9
2	10,14,15,16,17,18,19,20,21,22,23,24,25,26,27,29,30	0	93.5

Table 6- Results for Different Type of GA and PSO

Method	Objects of Goal Function			SVC		TCSC		Time ¹ (second)
	ATC (MW)	Average of Voltage Profile	Active Power Loss (MW)	Bus # for Location	Capacity (MVar)	Line for Location	Level of Compensation (pu)	
BGA	120.7867	1.0083	18.2520	4	83.668	4-15	0.6	3342.250
RGA	122.9	1.0003	19.3227	7	92.963	27-28	0.6	3123.188
HRGA	100.94	1.0021	14.3783	30	7.6939	1-2	0.6	3430.453
PSO	116.9	0.9944	18.7453	7	74.2872	4-15	0.4983	3920.527
MPSO	123.18	1.0004	19.3258	7	93.0422	27-28	0.5966	3878.453
HMPSO	113.7	1.0261	14.228	12	48.7214	1-2	0.6	3728.937

Table 7-IEEE 57-Bus Areas Characteristics

Area	Bus numbers	Generation (MW)	Load (MW)
1	1-2-3-6-8-9-12	1283.6	822
2	Other buses except mentioned buses	0	428.8

¹ The CPU clock speed is 2.81 GHZ and RAM capacity is 256 MB

Table 8-Loadability of Each Tie-line Before Voltage Collapse

From Bus Number	To Bus Number	Flow (MW)	
		Without FACTS Devices	With FACTS Devices
3	4	36.722	85.538
4	6	3.8772	20.177
5	6	4.2	1.0336
7	8	76.863	97.632
9	55	8.8433	32.161
9	13	7.2553	1.0036
9	11	14.3	19.935
9	10	15.107	18.648
10	12	7.1923	31.526
12	17	34.608	68.679
1	17	76.373	120.87
1	16	62.974	105.04
3	15	16.146	38.826
1	15	130.28	228.39
12	16	20.233	51.899